14th European Signal Processing Conference (EUSIPCO 2006), Florence, Italy, September 4-8, 2006, copyright by EURASIP

NEW RECURSIVE ADAPTIVE BEAMFORMING ALGORITHMS FOR UNIFORM CONCENTRIC CIRCULAR ARRAYS WITH FREQUENCY INVARIANT CHARACTERISTICS

H. H. Chen, S. C. Chan, and K. L. Ho
Department of Electrical and Electronic Engineering
The University of Hong Kong, Pokfulam Road, Hong Kong

***Abstract*—**This paper proposes new recursive adaptive beamforming algorithms for uniform concentric circular array (UCCA) that has nearly frequency invariant (FI) characteristics. By using a fixed compensation network, the far field pattern of a UCCA frequency invariant beamformer (FIB) is determined by a set of weights and it is approximately invariant over a wide range of frequencies. New recursive adaptive beamforming algorithms based on the least mean square (LMS) and recursive least square (RLS) algorithms and the Generalized Sidelobe Canceller (GSC) structure are proposed to address the high computational complexity of the sample matrix inversion (SMI) method proposed previously by the authors. Simulation results show that the proposed adaptive FI-UCCA beamformer requires much fewer variable taps than the conventional UCCA for the same steady-state performance, while offering much faster convergence speed.

I. INTRODUCTION

Beamforming using sensor arrays is an effective method for suppressing interferences whose angles of arrival are different from the desired looking direction. They find important applications in radio communications, sonar, radar, and acoustics [1]-[3]. Traditional adaptive broadband beamformer usually employs tapped-delay lines or linear transversal filters with adaptive coefficients to generate appropriate beam patterns for suppressing undesirable interference. This usually requires considerable number of adaptive coefficients resulting in a rather long convergence time and high implementation complexity. These problems can be remedied by using subband decomposition technique, partial adaptation or using frequency invariant beamformers (FIB) [4]-[7], [9]. In FIB, a beam-forming network is used to generate beam pattern with approximately frequency invariant (FI) characteristics over the frequency band of interest. They can attenuate broadband directional interference using an adaptive beamformer with very few number of adaptive filter coefficients [5]. One of the widely studied FIB is the uniform linear array (ULA) FIB [4]-[8]. Due to the geometry of ULA, its angular resolution at boresight is better than that at its end-fire. In addition, it allows many efficient direction-of-arrival (DOA) detection algorithms to be developed. For example, the MUSIC algorithm [10] provides a high resolution method for detecting the angle of arrival (AoA) of the signal sources based on the subspace approach. The MUSIC algorithm is also applicable to DOA estimation of wideband coherent sources by performing the algorithm in beamspace using ULA-FIB [9]. Besides AoA estimation of wideband sources, adaptive interference suppression using beamspace adaptive beamforming [5] is also very attractive because of the small number of adaptive coefficients required and the possibility of employing partial adaptation, yielding faster convergence and fewer number of high speed variable multipliers.

Recently, electronic steerable uniform-circular arrays (UCAs) [11] with frequency invariant characteristics were studied in [12], where a fixed beamforming network is used to compensate for the frequency dependence of the array. Unfortunately, the passband of a UCA is rather narrow because it is closely related to its radius of the array. To obtain a frequency invariant characteristic over a large bandwidth, uniform concentric circular arrays (UCCA) are proposed in [13] and [14]. The basic idea of the FI UCCA is to transform each snapshot sampled by the array to the phase modes via an Inverse Discrete Fourier Transform (IDFT). The transformed data is then filtered to compensate for the frequency dependence of the phase modes. Finally, these frequency invariant phase-modes are linear combined using a set of weights or coefficients to obtain the desired frequency invariant beam patterns. These weights, which govern the far field pattern of the UCCA, can be designed by conventional 1D digital filter design techniques such as the Parks-McClellan algorithm to form fix beam patterns. Alternatively, these coefficients can be varied by an adaptive algorithm to form an adaptive beamformer with approximately frequency invariant characteristics. The compensation filters in the fixed beamforming network are designed using second order cone programming (SOCP) [16][17]. In [14], adaptive beamforming of FI-UCCA using the sample matrix inversion (SMI) method was studied and satisfactory performance was obtained. One disadvantage of the SMI method, however, is the high computational complexity, since it requires the inversion of the autocorrelation matrix. In this paper, new recursive beamforming algorithms for the FI-UCCA based on the least mean square (LMS) and recursive least square (RLS) algorithms and the Generalized Sidelobe Canceller (GSC) [19] structure were developed. A conventional tapped-delay line based adaptive UCCA beamformer without using the compensation network is also developed. Simulation results show that by using one tap per phase mode in the proposed adaptive UCCA-FIB, much faster convergence than the conventional UCCA adaptive beamformers can be achieved. Also, the performance of the latter levels off when the length of the tapped-delay line is increased beyond 10. After which, the performances are comparable to the one-tap FI-UCCA beamformer. In other words, the proposed adaptive FI-UCCA beamformer requires much fewer variable taps than the conventional UCCA. The paper is organized as follows: Sections II briefly reviewed the principle and design of the broadband FI-UCCA. The proposed broadband adaptive beamforming algorithms using the FI-UCCA are presented in section III. Design examples and simulation results of the broadband beamforming using the proposed UCCA are given in Section IV. Conclusions are drawn in Section V.

II. FI UNIFORM CONCENTRIC CIRCULAR ARRAYS

The structure and design of the frequency invariant uniform concentric circular array (FI-UCCA) [13], [14] is briefly reviewed in this section. Figure 1 shows the geometry of a UCCA with P rings and each ring has K_p omnidirectional sensors located at $\{r_p\cos\phi_{k_p}, r_p\sin\phi_{k_p}\}$ (represented as Cartesian Coordinate with the center as the origin) where r_p is the radius of the p^{th} ring, $p=1,\cdots,P$, $\phi_{k_p}=2\pi k_p/K_p$ and $k_p=0,\cdots,K_p-1$ as shown in Figure 2. In UCCAs, the inter-sensor spacing in each ring is fixed at $\lambda/2$ where λ is the smallest wavelength of the array to be operated and is denoted by λ_s. The radius of the p^{th} ring of the UCCA is given by

$$r_p=\lambda_s/(4\sin(\pi/K_p)). \quad (1)$$

For convenience, this radius is represented as its normalized version $\hat{r}_p=r_p/\lambda_s=1/(4\sin(\pi/K_p))$. The steering vector of the

p^{th} ring of a UCCA can be written as:

$$\boldsymbol{a}_p(\omega,\phi)=[e^{j\omega\hat{r}_p\alpha\sin\theta\cos(\phi-\phi_0)}\ \ e^{j\omega\hat{r}_p\alpha\sin\theta\cos(\phi-\phi_1)}\cdots e^{j\omega\hat{r}_p\alpha\sin\theta\cos(\phi-\phi_{K_p-1})}]^T, \quad (2)$$

where $\alpha=f_s/f_{\max}$ denotes the ratio of the sampling frequency f_s to the maximum frequency $f_{\max}$, θ is the elevation angle that is measured from a reference imaginary axis perpendicular to the horizontal plane, ϕ is the azimuth angle measured from a reference imaginary axis on the horizontal plane of the sensors. The UCCA employed in this paper has an elevation angle of $\theta=\pi/2$, i.e. on the horizontal plane.

The structure of the FI-UCCA beamformer is shown in Figure 3. After appropriate down-conversion, lowpass filtering and sampling, the sampled signals of the p^{th} ring from the antennas are given by the vector $\boldsymbol{X}_p[n]=[x_0^{(p)}[n]\ x_1^{(p)}[n]\cdots x_{K_p-1}^{(p)}[n]]^T$, which is called a snap-shot at sampling instance *n*. Each snapshot is IDFT transformed to obtain the phase-mode signal $V_{m_p}^{(p)}[n]$, $m_p=-L_p,...,L_p$, $p=1,\ldots,P$. Each phase mode is then filtered or compensated by a compensation filter with impulse response $\boldsymbol{h}_{m_p}^{(p)}(n)$. The compensated signals are then inputted to the adaptive beamforming network to form the output of the entire adaptive UCCA-FIB. Since the compensated phase mode signals are relatively frequency invariant in the desired frequency band, very few taps are required in the subsequent adaptive beamforming network for extracting the desired signals and suppressing the interferences. In our simulations, one tap per phase mode is found to give satisfactory performance. In other words, the adaptive beamforming network is working like a narrowband adaptive beamformer. The detail derivation of the spatial-frequency response of the UCCA was discussed in [13] and [14]. Due to space limitation, we only give the response of the array as follows:

$$G(\omega,\phi)=\sum_{m=-L_P}^{L_P}g_m\cdot e^{jm\phi}\cdot\left[\sum_{p=1}^{P}K_p j^m J_m(\omega\hat{r}_p\alpha)\cdot H_m^{(p)}(\omega)\right], \quad (3)$$

where $J_m(\cdot)$ is the Bessel function of the first kind and $H_m^{(p)}(\omega)$ is the frequency response of the compensation filter in the m^{th} phase mode, g_m is the spatial weight coefficient and K_p is the number of sensors in the p^{th} ring. From (3), it can be seen that if the filters $H_m^{(p)}(\omega)$ are designed in such a way that

$$\sum_{p=1}^{P}K_p j^m J_m(\omega\hat{r}_p\alpha)\cdot H_m^{(p)}(\omega)\approx 1 \text{ for } \omega\in[\omega_L,\omega_U], \quad (4)$$

where ω_L and ω_U are respectively the lower and upper frequencies of interest, then the beamformer in (4) will be approximately frequency invariant within $\omega\in[\omega_L,\omega_U]$ and

$$G(\omega,\phi)\approx\sum_{m=-L_P}^{L_P}g_m e^{jm\phi}. \quad (5)$$

From this equation, we can see that the far field beam pattern is now governed by the spatial weighting $\{g_m\}$ alone and it can be written as $G(\omega,\phi)\approx G(\phi)$, which is similar to that of a digital FIR filter with impulse response $\{g_m\}$. The real-time adaptation of the beam pattern through the spatial weighting $\{g_m\}$ to suppress undesired interference is simpler than traditional broadband adaptive arrays using tapped delay lines as we will see later in section IV.

Since the left hand side of (4) is a linear function of the filter coefficients in $H_m^{(p)}(\omega)$'s, the design problem in (4) can be treated as a digital FIR filter design problem with all the filter outputs adding up to the desired response, which is equal to one. If the minimax error criterion is used, the filter coefficients for $H_m^{(p)}(\omega)$ can be determined by second order cone programming (SOCP) [16]. SOCP is a convex programming problem and the global optimal solution is guaranteed if it exists. Another important advantage of SOCP is that it is very convenient to include additional linear or convex quadratic constraints, such as the norm constraints of the variable vector, to the design problem. It has been used in the optimal design of digital FIR filters and fixed beam broadband ULA FIBs [15]. Due to page limitation, the details of the design method are omitted here. Interested readers can refer to[13][14] for more information.

III. ADAPTIVE BEAMFORMING USING UCCA FIB

The FI-UCCA designed in the previous section can be used in broadband adaptive beamforming. With the FI characteristic, the length of the variable weight vector in the beamformer can be significantly reduced compared to conventional UCCAs without employing the compensation network. Now we consider *I* broadband signals $s_i[n]$, i=1,…,I, which impinge a *P*-ring UCCA respectively at azimuth angles ϕ_i, i=1,…,I. The frequency response of the output signal can be written as:

$$Y(\omega)=\sum_{m=-L_P}^{L_P}g_m\left[\boldsymbol{a}_{G_m}(\Phi,\omega)\boldsymbol{S}(\omega)+N_m(\omega)\right], \quad (6)$$

where $\boldsymbol{S}(\omega)=[S_1(\omega),...,S_I(\omega)]^T$ is the frequency response of the I incoming signals, $\boldsymbol{a}_{G_m}(\Phi,\omega)=[a_{G_m}(\phi_1,\omega),...,a_{G_m}(\phi_I)]$ is the spatial-frequency response of the FI-UCCA array in the m^{th} phase mode that evaluated at the angles of ϕ_i, i=1,…,I and $N_m(\omega)$ is the frequency response of the sensor noise that is transformed to phase mode. From (3) and (4), we know that $\boldsymbol{a}_{G_m}(\Phi,\omega)$ is designed to be frequency invariant and hence $a_{G_m}(\phi,\omega)\approx a_{G_m}(\phi)$, $\omega\in[\omega_l,\omega_u]$. Thus, the frequency response of the beamformer output is simplified to:

$$Y(\omega)\approx\sum_{m=-L_P}^{L_P}g_m[\boldsymbol{a}_{G_m}(\Phi)\boldsymbol{S}(\omega)+N_m(\omega)]. \quad (7)$$

For notation convenience, we shall replace the approximation sign by the equality sign and assume that the errors are absorbed into the sensor noise terms $N_m(\omega)$. Taking the IDFT, one gets the time-domain expression of the output as follows:

$$y[n]=\sum_{m=-L_P}^{L_P}g_m[\boldsymbol{a}_{G_m}(\Phi)\boldsymbol{s}[n]+\eta_m[n]]=\sum_{m=-L_P}^{L_P}g_m y_{CPM\_m}[n], \quad (8)$$

where $\eta_m[n]$, with FT $N_m(\omega)$, is the output noise of the m^{th} phase mode of the beamformer, and $y_{CPM\_m}[n]$ is the m^{th} compensated phase mode signal. To be consistent with the literature, let the weight vector $\boldsymbol{g}=\boldsymbol{w}=[w_1,\cdots,w_M]^T$, the beamforming output can be written as:

$$y[n]=\boldsymbol{w}^H\boldsymbol{y}_{CPM}[n]=\boldsymbol{w}^H\boldsymbol{a}_G(\Phi)\cdot\boldsymbol{s}[n]+\boldsymbol{w}^H\boldsymbol{\eta}_{CPM}[n] \quad (9)$$

where $\boldsymbol{a}_G(\Phi)=[\boldsymbol{a}_{G_{-L_p}}(\Phi),\cdots,\boldsymbol{a}_{G_{L_P}}(\Phi)]^T$ is the $(M\times I)$ source direction matrix with $\boldsymbol{a}_{G_m}(\Phi,\omega)\approx\boldsymbol{a}_{G_m}(\Phi)$ given by (6). $\boldsymbol{y}_{CPM}[n]=[y_{CPM\_-L_P}[n],\cdots,y_{CPM\_L_P}[n]]^T$ is the compensated phase mode vector, and $\boldsymbol{\eta}_{CPM}[n]=[\eta_{CPM\_-L_P}[n],\cdots,\eta_{CPM\_L_P}[n]]^T$ is the noise vector containing the noises at the compensated phase modes of the beamformer.

Assume that the desired signal impinges the array at an azimuth angle ϕ_d. To recover the desired signal from the array output, we firstly employ the classical Minimum Variance Beamformer (MVB) [17] (or minimum variance distortion-less response MVDR beamformer). The basic idea of MVB is to choose the weight vector $\boldsymbol{w}$ such that the output energy of the

array is minimized, while requiring the response of the array in the looking direction to be 1, hence the name MVDR. The MVDR problem that employing FI-UCCA can be written as:

$$\text{minimize } \boldsymbol{w}^H \boldsymbol{R}_{y\_CPM} \boldsymbol{w} \quad (10)$$

$$\text{subject to } \boldsymbol{w}^H \boldsymbol{a}_G(\phi_d) = 1,$$

where $\boldsymbol{R}_{y\_CPM} = E\{\boldsymbol{y}_{CPM}[n] \cdot \boldsymbol{y}_{CPM}^H[n]\}$ is the auto-correlation of the data matrix. This constrained optimization can be solved analytically and the optimal solution is:

$$\boldsymbol{w}_{opt} = \boldsymbol{R}_{y\_CPM}^{-1} \boldsymbol{a}_G(\phi_d) / (\boldsymbol{a}_G^H(\phi_d) \boldsymbol{R}_{y\_CPM}^{-1} \boldsymbol{a}_G(\phi_d)). \quad (11)$$

Given a series of snapshots $\boldsymbol{y}_{CPM}[n]$, say n=1,…,K, the autocorrelation matrix can be estimated as $\hat{\boldsymbol{R}}_{y\_CPM} = \sum_{n=1}^{K} \boldsymbol{y}_{CPM}[n] \boldsymbol{y}_{CPM}^H[n]$. Thus, $\boldsymbol{w}_{opt}$ can be obtained by inverting the matrix $\hat{\boldsymbol{R}}_{y\_CPM}$ and substituting it into the right hand side of (11). This is called the sample matrix inversion (SMI) method.

As mentioned earlier, adaptive beamforming using SMI method and the FI-UCCA was studied in [14]. The SMI method, however, is very computational expensive because it requires the inversion of the autocorrelation matrix. Alternatively, the weight vector $\boldsymbol{w}$ can be solved recursively using adaptive filtering algorithms such as the Least Mean Squares (LMS) algorithm and the recursive least squares (RLS) algorithm using a structure called Generalized Sidelobe Canceller (GSC) [18]. Figure 4 shows the structure of the GSC-based beamformer. The weighting vector $\boldsymbol{w}$ is decomposed into two parts: the fixed part $\boldsymbol{w}_c$ and the adaptive part $\boldsymbol{w}_a$. The fixed weight vector $\boldsymbol{w}_c$, as shown in the upper part in Figure 4, forms a main beam that is steered towards some assumed propagation direction. It can be obtained as:

$$\boldsymbol{w}_c = \boldsymbol{a}_G(\phi_d)[\boldsymbol{a}_G^H(\phi_d)\boldsymbol{a}_G(\phi_d)]^{-1} \boldsymbol{a}_G^H(\phi_d). \quad (12)$$

Normally, the beam is designed to have a looking direction at zero degree and the desired looking direction is obtained by delaying the sensor inputs appropriately. In the proposed FI-UCCA, since the direction of the beam can be readily changed by modulating the beam weight $\{g_m\}$ with an appropriate sinusoid, these delay elements are unnecessary. The adaptive part $\boldsymbol{w}_a$ is continuously updated in order to remove any undesired signals other than the looking direction from appearing at the array output. A blocking matrix $\boldsymbol{B}$ is first employed to block or prevent the desired signal at the looking direction from entering the adaptive part. Consequently, the input to the adaptive part mainly consists of the undesirable signals. The interference signal, after modifying by the adaptive weight vector $\boldsymbol{w}_a$, is then subtracted from the main beam in order to cancel the interference that is present in the main beam. This is achieved by minimizing the output energy of the beamformer using either the RLS or LMS adaptive filtering algorithms. In the LMS algorithm, the weight vector $\boldsymbol{w}_a$ is updated in the following way:

$$\boldsymbol{w}_a[n] = \boldsymbol{w}_a[n-1] + \mu \cdot y^*[n] \boldsymbol{B} \boldsymbol{y}_{CPM}[n], \quad (13)$$

where μ is a stepsize parameter. Alternatively, if the RLS filtering algorithm is used, the weight vector is updated as:

$$\boldsymbol{w}_a[n] = \boldsymbol{w}_a[n-1] + \boldsymbol{K}_M y^*[n], \quad (14)$$

where $\boldsymbol{K}_M[n] = \dfrac{\boldsymbol{P}[n-1]\boldsymbol{B}\boldsymbol{y}_{CPM}[n]}{\lambda + (\boldsymbol{B}\boldsymbol{y}_{CPM}[n])^H \boldsymbol{P}[n-1](\boldsymbol{B}\boldsymbol{y}_{CPM}[n])}$ is the Kalman gain, $\boldsymbol{P}[n]$ is the inverse of the autocorrelation matrix and it can be updated as $\boldsymbol{P}[n] = \lambda^{-1}(\boldsymbol{P}[n-1] - \boldsymbol{K}_M[n](\boldsymbol{B}\boldsymbol{y}_{CPM}[n])^H \boldsymbol{P}[n-1])$ with $\boldsymbol{P}[0] = \frac{1}{\delta^2}\boldsymbol{I}$, δ^2 is a small number to ensure that $\boldsymbol{P}[0]$ is non-singular initially and λ is the forgetting factor that controls the tracking ability and steady state error of the RLS algorithm.

IV. SIMULATION RESULTS

We now evaluate, by computer simulation, the performance of the adaptive FI-UCCA in real-time beamforming using the LMS-GSC and RLS-GSC algorithms described previously. The FI-UCCA used in this example has two rings. The inner ring and the outer ring have 10 and 18 omni-directional sensors, respectively. The required bandwidth of the UCCA-FIB is $\omega \in [0.2\pi, 0.65\pi]$. The numbers of phase modes M of the inner and outer rings are respectively 9 and 17. The desired beam is targeted at 0^o and the beamwidth is 10^o. The spatial-frequency response is shown in Figure 5. We can see that the beamformer is approximately frequency invariant.

The desired signal and the incoherent interfering signal are assumed to impinge the array at angles 0º and 50º, respectively. The desired signal is composed of 53 sinusoidal signals with frequencies ranging from 0.8×10^8 to 6×10^8 Hz at an interval of 0.1×10^8 Hz. The interfering signal is also composed of 53 sinusoidal signals but with frequencies ranging from 0.83×10^8 to 6.3×10^8 Hz at an interval of 0.1×10^8 Hz. The SIR is -20 dB. The additive white Gaussian noise at each sensor is assumed to have the same power and the SNR is 20 dB.

The stepsize of the LMS algorithm is set to 0.015. The line labeled *LMS* in Figure 6 plots the output MSE between the beamforming output and the desired signal. The *x*-axis is the iteration number. The forgetting factor of the RLS algorithm is set to 0.999, and the output MSE of the RLS algorithm is also shown in Figure 6 with the line labeled *RLS*. The MSE outputs are obtained by averaging 200 independent trials and it is further averaged on the snapshots with a window length of 300. The number of the tap per phase mode is one in both algorithms. We can see that with the same steady state error, the LMS algorithm converges at around 3000 snapshot and the RLS algorithm converges at around 1500 snapshot. The line labeled *SMI* is the simulation results for the SMI method. For comparison, we also simulated the performance of a conventional beamformer using the UCCA without the compensation network. The lines labeled *UCCA 1 tap-SMI* and *UCCA 1 tap-LMS* are the output MSEs of the beamformers using SMI and LMS algorithms, respectively. The error of the SMI algorithm is much higher than that of the one-tap FI-UCCA and the convergence of the LMS algorithm is much slower, which converges at around the 2×10^4 snapshot. The output MSE of the UCCA decreases as the length of the tapped-delay line is increased and it levels off when the length of the tapped-delay line is increased beyond 10. For illustrative purpose, the corresponding output MSE is plotted in Fig. 6 as the line labeled *UCCA 10 taps-SMI*. The results of using the LMS and RLS algorithms are very slow and it is omitted to save space.

V. CONCLUSION

New broadband recursive adaptive beamforming algorithms for FI uniform concentric circular array (UCCA) are presented. The algorithms are based on the least mean square (LMS) and recursive least square (RLS) algorithms, and the Generalized Sidelobe Canceller (GSC) structure. Simulation results show that the proposed adaptive FI-UCCA beamformer requires much fewer variable taps than the conventional UCCA for the same steady-state performance, while offering much faster convergence speed.

References

[1] D. H. Johnson and D. E. Dudgeon, *Array signal processing: concepts and techniques*, Prentice Hall, 1993.

[2] H. Krim and M. Viberg, "Two decades of array signal processing research: the parametric approach," *IEEE Signal Processing Mag.*, vol. 13, pp. 67-94, Jul. 1996.

[3] B. D. Van Veen and K. M. Buckley, "Beamforming: a versatile approach to spatial filtering," *IEEE ASSP Mag.*, vol. 52, pp. 4-24, Apr. 1988.

[4] K. Nishikawa, T. Yamamoto, K. Oto and T. Kanamori, "Wideband beamforming using fan filter," in *Proc. IEEE ISCAS,* vol. 2., pp. 533-536, 1992.

[5] T. Sekiguchi and Y. Karasawa, "Wideband beamspace adaptive array utilizing FIR Fan filters for multibeam forming," *IEEE Trans. Signal Processing*, vol. 48, pp. 277-284, Jan. 2000.

[6] D. B. Ward, R. A. Kennedy and R. C. Williamson, "Theory and design of broadband sensor arrays with frequency invariant far-field beam patterns," *J. Acoust. Soc. Amer.*, vol. 97, no.2, pp.1023-1034, Feb. 1995.

[7] D. B. Ward, R. A. Kennedy and R. C. Williamson, "FIR filter design for frequency invariant beamformers," *IEEE Signal Processing Lett.*, vol.3, pp. 69-71, Mar. 2000.

[8] M. Ghavami and R. Kohno, "Recursive fan filters for a broad-band partially adaptive antenna," *IEEE Trans. Commun.*, vol. 48, pp.185-188, Feb. 2000.

[9] D. B. Ward, Z. Ding and R. A. Kennedy, "Broadband DOA estimation using frequency invariant beamforming," *IEEE Trans. Signal Processing*, vol. 46, pp. 1463-1469, May 1998.

[10] R. O. Schmidt, "Multiple emitter location and signal parameter estimation," *IEEE Trans. Antennas Propagat.*, vol. AP-34, pp. 276-280, Mar. 1986.

[11] H. Steyskal, "Circular array with frequency-invariant pattern," *Antennas and Propagation Society International Symposium 1989*, AP-S. Digest, vol. 3, pg. 1477-1480, 1989.

[12] S. C. Chan and Carson K. S. Pun, "On the design of digital broadband beamformer for uniform circular array with frequency invariant characteristics," *IEEE ISCAS2002*, vol. 1, pp. 693-696, May 2002.

[13] S. C. Chan and H. H. Chen, "Theory and design of uniform concentric circular Arrays with frequency invariant characteristics", *IEEE ICASSP'05*, vol. 4, pp. 805-808, Mar. 2005.

[14] S. C. Chan, H. H. Chen and K. L. Ho, "Adaptive beamforming using uniform concentric circular arrays with frequency invariant characteristics", *IEEE ISCAS'05*, pp. 4321- 4324, May 2005.

[15] J. O. Coleman and D. P. Scholnik, "Design of nonlinear phase FIR Filters with second-order cone programming," in *Proc. IEEE MWSCAS*, vol. 1, pp. 409-412, 1999.

[16] M. S. Lobo, L. Vandenberghe, S. Boyd and H. Lebret, "Applications of second-order cone programming", *Linear Algebra Application*, vol. 248, pp.193-228, Nov. 1998.

[17] J. Capon, "High-resolution frequency-wavenumber spectrum analysis," *Proc. IEEE*, vol. 57, no. 8, pp. 1408-1418, August 1969.

[18] K. M. Buckley and L. J. Griffiths, "An adaptive generalized side-lobe canceller with derivative constraints," *IEEE Trans. on Antenn-as and Propagation*, vol. AP-34, No. 3, pp. 311-319, March 1986.

[19] L. J. Griffiths and C. W. Jim, "An alternative approach to linearly constrained adaptive beamforming", *IEEE Transactions on Antennas and Propagation*, vol. AP-30, No. 1, pp. 27-34, Jan. 1982.

Figures

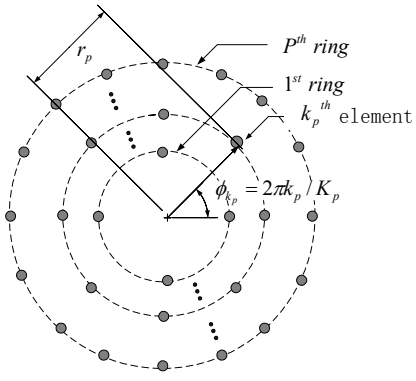

Figure 1. A UCCA with P rings and K_p-sensor at each ring.

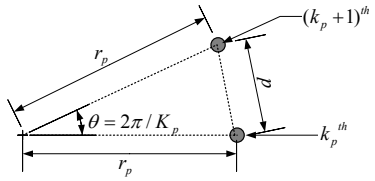

Figure 2. Relationship between inter-sensor spacing and the radius of the p^{th} ring of the UCCA.

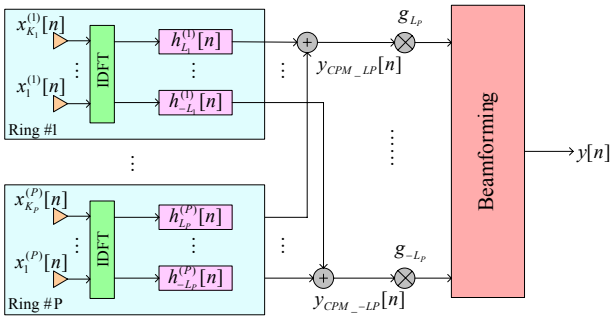

Figure 3. The block diagram of a P-ring UCCA-FIB.

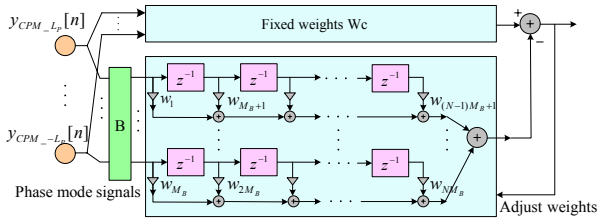

Figure 4. The structure for GSC beamformer.

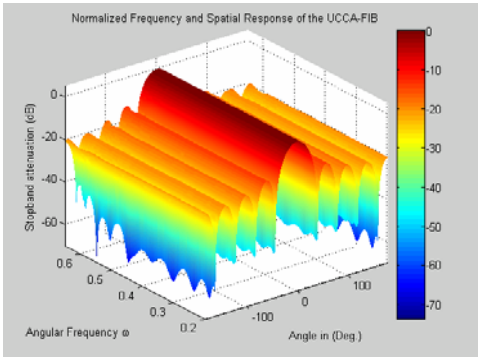

Figure 5. Spatial response and frequency response of the UCCA-FIB.

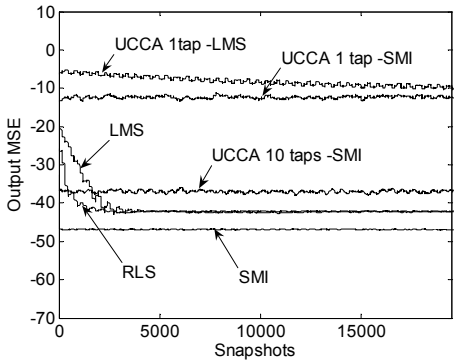

Figure 6. The output errors of the adaptive beamformers using FI-UCCA and conventional UCCA.